Aung, Tin, Ozaki, Mineo, Mizoguchi, Takanori, Allingham, R. Rand, Li, Zheng, Haripriya, Aravind, Nakano, Satoko, Uebe, Steffen, Harder, Jeffrey M., Chan, Anita S. Y., Lee, Mei Chin, Burdon, Kathryn P., Astakhov, Yury S., Abu-Amero, Khaled K., Zenteno, Juan C., Nilgün, Yildirim, Zarnowski, Tomasz, Pakravan, Mohammad, Safieh, Leen Abu, Jia, Liyun, Wang, Ya Xing, Williams, Susan, Paoli, Daniela, Schlottmann, Patricio G., Huang, Lulin, Sim, Kar Seng, Foo, Jia Nee, Nakano, Masakazu, Ikeda, Yoko, Kumar, Rajesh S., Ueno, Morio, Manabe, Shin-ichi, Hayashi, Ken, Kazama, Shigeyasu, Ideta, Ryuichi, Mori, Yosai, Miyata, Kazunori, Sugiyama, Kazuhisa, Higashide, Tomomi, Chihara, Etsuo, Inoue, Kenji, Ishiko, Satoshi, Yoshida, Akitoshi, Yanagi, Masahide, Kiuchi, Yoshiaki, Aihara, Makoto, Ohashi, Tsutomu, Sakurai, Toshiya, Sugimoto, Takako, Chuman, Hideki, Matsuda, Fumihiko, Yamashiro, Kenji, Gotoh, Norimoto, Miyake, Masahiro, Astakhov, Sergei Y., Osman, Essam A., Al-Obeidan, Saleh A., Owaidhah, Ohoud, Al-Jasim, Leyla, Shahwan, Sami Al, Fogarty, Rhys A., Leo, Paul, Yetkin, Yaz, Oğuz, Çilingir, Kanavi, Mozhgan Rezaei, Beni, Afsaneh Nederi, Yazdani, Shahin, Akopov, Evgeny L., Toh, Kai-Yee, Howell, Gareth R., Orr, Andrew C., Goh, Yufen, Meah, Wee Yang, Peh, Su Qin, Kosior-Jarecka, Ewa, Lukasik, Urszula, Krumbiegel, Mandy, Vithana, Eranga N., Wong, Tien Yin, Liu, Yutao, Koch, Allison E. Ashley, Challa, Pratap, Rautenbach, Robyn M., Mackey, David A., Hewitt, Alex W., Mitchell, Paul, Wang, Jie Jin, Ziskind, Ari, Carmichael, Trevor, Ramakrishnan, Rangappa, Narendran, Kalpana, Venkatesh, Rangaraj, Vijayan, Saravanan, Zhao, Peiquan, Chen, Xueyi, Guadarrama-Vallejo, Dalia, Cheng, Ching Yu, Perera, Shamira A., Husain, Rahat, Ho, Su-Ling, Welge-Luessen, Ulrich-Christoph, Mardin, Christian, Schloetzer-Schrehardt, Ursula, Hillmer, Axel M., Herms, Stefan, Moebus, Susanne, Nöthen, Markus M., Weisschuh, Nicole, Shetty, Rohit, Ghosh, Arkasubhra, Teo, Yik Ying, Brown, Matthew A., Lischinsky, Ignacio, Crowston, Jonathan G., Coote, Michael, Zhao, Bowen, Sang, Jinghong, Zhang, Nihong, You, Qisheng, Vysochinskaya, Vera, Founti, Panayiota, Chatzikyriakidou, Anthoula, Lambropoulos, Alexandros, Anastasopoulos, Eleftherios, Coleman, Anne L., Wilson, M. Roy, Rhee, Douglas J., Kang, Jae Hee, May-Bolchakova, Inna, Heegaard, Steffen, Mori, Kazuhiko, Alward, Wallace L. M., Jonas, Jost B., Xu, Liang, Liebmann, Jeffrey M., Chowbay, Balram, Schaeffeler, Elke, Schwab, Matthias, Lerner, Fabian, Wang, Ningli, Yang, Zhenglin, Frezzotti, Paolo, Kinoshita, Shigeru, Fingert, John H., Inatani, Masaru, Tashiro, Kei, Reis, André, Edward, Deepak P., Pasquale, Louis R., Kubota, Toshiaki, Wiggs, Janey L., Pasutto, Francesca, Topouzis, Fotis, Dubina, Michael, Craig, Jamie E., Yoshimura, Nagahisa, Sundaresan, Periasamy, John, Simon W. M., Ritch, Robert, Hauser, Michael A., & Khor, Chiea-Chuen
(2015)

HHS Public Access

Author manuscript

Nat Genet. Author manuscript; available in PMC 2015 October 14.

Published in final edited form as:

Nat Genet. 2015 April ; 47(4): 387–392. doi:10.1038/ng.3226.

A common variant mapping to *CACNA1A* is associated with susceptibility to Exfoliation syndrome

A full list of authors and affiliations appears at the end of the article.

Abstract

Exfoliation syndrome (XFS) is the commonest recognizable cause of open angle glaucoma worldwide. To better understand the etiology of XFS, we conducted a genome-wide association study (GWAS) on 1,484 patients and 1,188 controls from Japan, and followed up the most significant findings on a further 6,901 patients and 20,727 controls from 17 countries across 6 continents. We discovered a significant association between a new locus (*CACNA1A* rs4926244) and increased susceptibility to XFS (Odds ratio [OR] = 1.16, $P = 3.36 \times 10^{-11}$). Although overwhelming association at the *LOXL1* locus was confirmed, the key SNP marker (*LOXL1* rs4886776) demonstrated allelic reversal depending on ethnic grouping (In Japanese: $OR_{A\text{-}allele} = 9.87$, $P = 2.13 \times 10^{-217}$; In non-Japanese: $OR_{A\text{-}allele} = 0.49$, $P = 2.35 \times 10^{-31}$). Our findings represent the first genetic locus outside of *LOXL1* which surpasses genome-wide significance for XFS, and provides insight into the biology and pathogenesis of the disease.

XFS is a generalized disorder of the extracellular matrix that manifests most conspicuously in the eye. The exfoliation material consists of cross-linked, amyloid-like fibrillar material and glycoproteins. Apart from ocular tissues, this material deposits around blood vessels

Correspondence should be addressed to T.A. aung_tin@yahoo.co.uk, or to C.C.K khorcc@gis.a-star.edu.sg.

*These authors contributed equally to this work

**These authors jointly supervised this work

[73]A full list of members and affiliations appears in the Supplementary Note

Author Contributions

T.A., M.O., & C.C.K. conceived the project. M.O., T.M., R.R.A., A.H., S.N., J.E.C., A.W.H., D.A.M., P.M., J.J.W., Y.S.A., J.C.Z., Y.N., T.Z., M.P.,L.J., Y.X.W., S.W., D.P., PG.S., Y.I., R.S.K., M.U., S.Manabe., K.H., S.Kazama., R.I., Y.M., K.Miyata., K.S., T.H., E.C., K.I., S.I., A.Y., M.Y., Y.K., M.A., T.O., T.Sakurai, T.Sugimoto, H.C., K.Y., S.Y.A., E.A.O., S.A.A-O., O.O., L.A-J, S.A.S., Y.Y., C.O., M.R.K., A.N.B., S.Y., E.L.A., E.K-J., U.L., P.C., R.M.R., A.Z., T.C., R.Ramakrishnan., K.N., R.V., P.Z., X.C., D.G-V., S.A.P., R.H., S-L.H., U-C.W-L., C.M., U.S-S., S.Moebus., N.Weisschuh., R.S., A.G., I.L., J.G.C., M.C., Q.Y., V.V., P.Founti., A.C., A.L., E.A., A.L.C., M.R.W., D.J.R., I.M-B., K.Mori, S.Heegaard., W.L.M.A., J.B.J., L.X., J.M.L., F.L., N.Wang., P.Frezzotti., S.Kinoshita, J.H.F., M.I., D.P.E., L.R.P., T.K., J.L.W., F.T., N.Y., & R.Ritch conducted patient recruitment and phenotyping. Z.L., S.U., M.K., K.P.B., M.A.B., J.J.W., Y.G., K.Y.T., L.H., W.Y.M., S.Q.P., B.Z., J.S., N.Z., Z.Y., & S.V. performed genotyping experiments. J.M.H., A.S.Y.C., M.C.L., E.N.V., G.R.H., & S.W.M.J. led and performed immunohistochemistry and immunofluorescence experiments. Z.L., K.P.B., R.A.F., P.L., K.K.A-A., L.A.S., L.H., K.S.S., J.N.F., M.N., F.M., N.G., M.M., S.U., M.K., Y.Y.T., J.H.K., A.E.A.K., S.Herms, Y.L., K.T., B.Z., J.S., N.Z., S.V., Z.Y., G.R.H., A.C.O., F.P., & A.G., performed analysis. E.N.V., T.Y.W., C.Y.C., A.M.H., M.M.N., B.C., E.S., M.S., & A.R. contributed genetic and genotyping data from control populations. The manuscript was drafted by C.C.K., with critical input from T.A., R.R.A., L.R.P., J.L.W., F.P., F.T., M.D., S.W.M.J., R.Ritch, and M.A.H. The manuscript was approved by all authors. C.C.K was responsible for obtaining financial support for this study.

URLs

Illumina, www.illumina.com; Sequenom, www.sequenom.com; Applied Biosystems, http://www.appliedbiosystems.com/; PLINK, http://pngu.mgh.harvard.edu/~purcell/plink/; R statistical program package, www.r-project.org; IMPUTE2, http://mathgen.stats.ox.ac.uk/impute/impute_v2.html

COMPETING FINANCIAL INTERESTS

The authors declare no competing financial interests.

particularly in association with elastic connective tissue, and could be found in other organs[1]. The build-up of exfoliation material deposits and pigment in the trabecular meshwork can damage this tissue and impede the drainage of aqueous humor from the eye thus resulting in elevated intraocular pressure and glaucomatous optic neuropathy. Exfoliation glaucoma is the most serious known complication of XFS[2].

The first GWAS on XFS was reported in 2007 and successfully identified *LOXL1* as a major susceptibility locus for XFS[3]. Since then, multiple studies have uniformly corroborated the association of genetic variants of *LOXL1* with XFS[4–21]. However, data from these studies showed associated alleles for *LOXL1* SNPs frequently undergo allelic reversal depending on ethnic group[22]. These findings suggest that complex genetic mechanisms are present for XFS pathogenesis, and the possibility that additional susceptibility loci for XFS remain to be identified. We assembled an international, multi-institutional collaborative effort across 6 continents comprising 17 countries to conduct a GWAS discovery and two-staged replication study of XFS (see **Methods**, Supplementary Table 1, and Supplementary Figure 1). Participating subjects provided written informed consent under the oversight of all local institutional review boards in accordance with the tenets of the Declaration of Helsinki.

For the GWAS discovery stage, we genotyped 717,991 SNP markers on 1,578 Japanese patients with XFS and 1,215 controls using the Illumina OmniExpress microarray. Control subjects were drawn from the same hospital where the XFS patients were first identified. A total of 1,484 cases and 1,188 controls passed quality control (QC) filters for call-rate, relatedness, heterozygosity and ancestry (see **Methods** for QC details) and were included for downstream association analysis. Multiple markers in strong linkage disequilibrium (LD) at the *LOXL1* locus showed strong evidence of association with XFS (Supplementary Figure 2a), with rs4886776 ($P = 7.37 \times 10^{-137}$) serving as the sentinel SNP.

A total of 66 SNPs outside of *LOXL1* showed evidence of association with XFS surpassing $P < 1 \times 10^{-4}$ at the GWAS discovery stage. We thus designed validation assays for these 66 SNP markers, together with *LOXL1* rs4886776, and genotyped them in a follow up collection of 2,628 XFS cases and 8,947 controls drawn from 9 countries (Stage 1 validation, see Supplementary Table 1). For each SNP examined, we conducted a fixed-effects meta-analysis to summarize the observations across the nine studies. One SNP marker (rs4926244), mapping within the *CACNA1A* gene that showed association in the GWAS discovery stage at $P = 5.50 \times 10^{-5}$ ($OR_{G\text{-allele}} = 1.29$) was also significant in this validation stage ($OR_{G\text{-allele}} = 1.17$, $P = 4.17 \times 10^{-5}$). Thus for rs4926244, meta-analysis of both the discovery and validation stages revealed genome-wide significant association ($OR_{G\text{-allele}} = 1.20$, $P = 2.45 \times 10^{-8}$) (Figure 1, Supplementary Table 2, and Supplementary Figure 2b). Results for all 67 SNP markers from the GWAS discovery and Stage 1 replication are appended in Supplementary Table 2. We did not observe consistent evidence of association at *CNTNAP2*, a locus previously reported to associate with XFS from a pooled GWAS study[23], as well as other previously reported candidate genes (Supplementary Table 3).

We subjected *CACNA1A* rs4926244 to further technical scrutiny in a third, independent dataset consisting of 4,273 XFS cases and 11,780 controls drawn from 8 additional countries

(Stage 2, replication; see Supplementary Table 1). The association maintained significance, consistent with findings observed in the two previous stages ($OR_{G\text{-allele}} = 1.13$, $P = 1.14 \times 10^{-4}$). Together, the combined discovery and two-stage replication patient collections consisting of 8,385 XFS cases and 21,915 controls provide evidence for association between the minor G allele at rs4926244 and XFS ($P = 3.36 \times 10^{-11}$). These data suggest risk for XFS increases approximately 1.16 fold for each copy of the minor G allele (Figure 1 and Supplementary Table 4). This association appears to be consistent with minimal heterogeneity when stratified for Asian ($OR_{G\text{-allele}} = 1.14$, $P = 7.46\times10^{-6}$), European ($OR_{G\text{-allele}}=1.19$, $P=1.90\times10^{-6}$) or South African ($OR_{G\text{-allele}} = 1.33$, $P = 0.11$)($P_{het} = 0.5$, $I^2 = 0\%$) ethnic groups (Figure 1).

SNP rs4926244 resides within an intronic region near the 3′ end of *CACNA1A*. It is flanked closely by recombination events (Figure 2) and is confined to its own linkage disequilibrium (LD) block (Supplementary Figure 3). We did not observe association with any genetic marker surpassing the nominal threshold of $P < 0.001$ outside of this critical region (Figure 2)[24]. We next performed imputation for unobserved SNPs at the *CACNA1A* locus on the basis of 1,000 Genomes cosmopolitan project data using the Phase 3 release (June 2014, see **Methods**) across the GWAS discovery collection. We were able to successfully impute 5602 SNPs across the *CACNA1A* locus. However, subsequent association analysis utilizing the imputed SNPs did not identify additional genetic associations that surpassed the statistical significance of rs4926244 (Supplementary Figure 4). Notably, the most significant SNPs emerging from the cosmopolitan imputation analysis are intronic and are all moderate-to-highly correlated with rs4926244 (Supplementary Table 5). None of these correlated SNP markers lies in strong motifs for transcription factor binding sites as identified by ENCODE. They also do not tag any common non-synonymous variants in *CACNA1A* (Supplementary Table 6). Haplotype association analysis assessing SNPs in a 2, 3, and 4 marker sliding window did not reveal evidence of association surpassing that observed for rs4926244 (lowest haplotype *P*-value = 0.00021; Supplementary Table 7), and we further note that all but one haplotype showing evidence of association exceeding $P < 0.0005$ in the GWAS dataset contained SNP rs4926244 (Supplementary Table 7). This suggests that rs4926244 is likely driving the common-variant haplotype association results, and that detailed fine-mapping of this locus using deep re-sequencing may be required. Examination of a recently available large-scale eQTL mapping database indicates the risk allele G at rs4926244 is modestly correlated with lower *CACNA1A* mRNA levels in peripheral blood cells ($Z=-3.00$, $P=0.0027$), suggesting that it may influence XFS risk through an effect on *CACNA1A* expression[25]. Further work will be needed to evaluate its effect in human ocular tissues.

Initial analysis of the *LOXL1* locus in the GWAS discovery dataset of Japanese descent demonstrated strong association at rs4886776 ($OR_{A\text{-allele}} = 8.31$, $P = 7.37 \times 10^{-137}$). The strength of this association vastly exceeded that of marker rs3825942 (responsible for a p.G153D substitution in exon 1 of *LOXL1*), which has been the most widely tested and reported SNP association prior to this analysis[22]. Performing the analysis after conditioning for the allele dosage of rs4886776 extinguished the signal of association for every other genetic marker within the *LOXL1* locus. Conversely, conditioning the analysis for allele dosage at rs3825942 still resulted in genome-wide significant association at many of the

other *LOXL1* SNPs, including rs4886776 (Supplementary Table 8). These data suggest that within the Japanese GWAS discovery set, the observed association at *LOXL1* can be attributed to rs4886776 alone. We note that rs4886776 is in high LD with rs1048661 (r^2=0.98 in 1000 genomes Asians), a SNP responsible for another non-synonymous substitution (p.R141L) in *LOXL1* but was not directly genotyped in our dataset. However, we were able to successfully impute rs1048661 in our GWAS discovery dataset and we confirmed strong association between it and XFS ($OR_{T\text{-allele}} = 8.13$, $P = 1.32 \times 10^{-126}$). SNP rs1048661 has been previously reported to show strong association with XFS in multiple populations, although the risk allele is reversed depending on which ethnic group is being studied[11,22]. This SNP is also in LD with several other *LOXL1* SNPs in potential transcription factor binding sites (Supplementary Table 6)[26,27].

Both rs4886776 and rs3825942 are in moderate pair-wise linkage disequilibrium ($r^2 = 0.23$). When we genotyped rs4886776 through the 2,628 XFS cases and 8,947 controls from Stage 1 validation (Supplementary Table 1), we noted very strong evidence of consistent association in the Japanese ($OR_{A\text{-allele}} = 21.7$, $P = 1.54 \times 10^{-135}$), leading to an overwhelmingly significant association in the Japanese cases and controls analyzed ($OR_{A\text{-allele}} = 9.87$, $P = 2.13 \times 10^{-217}$). Strikingly in non-Japanese, the direction of the association was opposite to that seen in the Japanese ($OR_{A\text{-allele}} = 0.49$, $P = 2.35 \times 10^{-31}$) (Supplementary Figure 5). Such a scenario echoes recently reported observations for the reversed effect of rs3825942 on XFS risk in South Africans, and suggests that the genetic mechanism whereby *LOXL1* exerts its effect on individual susceptibility to XFS is complex[22]. We failed to detect any evidence of statistically significant interaction between *CACNA1A* rs4926244 and the sentinel *LOXL1* polymorphisms, suggesting that both loci impact XFS risk via distinct biological pathways.

CACNA1A encodes for the alpha 1A subunit of the type P/Q voltage-dependant calcium channel. Calcium channels are responsible for the transport of calcium ions across cell membranes and play a key role in a cell's ability to generate and transmit electrical signals. Previous electron microscopy studies on human XFS eyes showed the presence of high calcium concentration in direct association with aggregating XFS fibrils[28]. In addition it is well known that fibrillin utilizes calcium to form stable aggregates[29]. Thus, it can be hypothesized that altered function of a calcium channel could lead to alterations of calcium concentrations that may facilitate the formation of XFS aggregates.

As there is a paucity of information on *CACNA1A* expression in the eye, we examined the mRNA expression profile and protein expression of *CACNA1A* from a variety of human ocular tissues and cell lines respectively (Supplementary Figure 6). *CACNA1A* mRNA expression was detected in all of the ocular tissues we studied with the exception of the optic nerve head (Supplementary Figure 6, panel A). Expression of different CACNA1A isoforms appear to be higher in human ocular tissue-derived cells than in cells of non-ocular origin (Supplementary Figure 6, panel B). Immunofluorescence and immunohistochemistry analysis was also performed on adult human eyes which showed positive immunoreactivity for CACNA1A in multiple human ocular tissues (Figure 3, Supplementary Figure 7 & 8). The distribution of CACNA1A was similar in human ocular tissues of individuals with or without XFS (Figure 3, Supplementary Figures 8 & 9). Positive staining and localization of

CACNA1A in the human eye was further corroborated by immunofluorescence microscopy analysis in mouse eyes. (Supplementary Figure 10). In the human eyes, we observed positive CACNA1A immunoreactivity in the ciliary body and iris (Figure 3). Positive staining of CACNA1A was also seen in the anterior lens epithelium but not in the acellular capsule and the cornea (Supplementary Figure 7 & 9). The optic nerve glia and vascular endothelial cells also showed positive immunoreactivity with CACNA1A (Supplementary Figure 9). In the retina, strong diffuse CACNA1A staining was seen in the photoreceptor inner segments (IS), inner nuclear layer (INL) and outer nuclear layer (ONL) and nerve fibre layer (NFL) of non XFS globes in comparison to the XFS globes where focal and patchy immunostaining of the IS, ONL, INL and NFL was observed. Light microscopy comparison of the irides in XFS eyes against non-XFS eyes showed typical XFS findings of exfoliated material on the posterior iris and atrophic iris pigment epithelium, as well as the possible atrophy of the iris dilator muscle in XFS eyes (Figure 3). Double immunofluorescence microscopy for CACNA1A and LOXL1 was also performed in human eyes with XFS and without XFS and showed co-localisation of CACNA1A and LOXL1 only in the epithelium of the ciliary processes. The exfoliated material in XFS eyes showed LOXL1 positive staining with negligible CACNA1A immunoreactivity. The ciliary body and iris smooth musculature had CACNA1A positive immunostaining but were negatively stained for LOXL1 in both XFS and non-XFS eyes (Figure 3). This observation raises the possibility that CACNA1A and LOXL1 contribute to XFS pathology through different mechanisms at different ocular sites.

In summary, we have identified a susceptibility locus mapping to *CACNA1A* using a three-staged GWAS study design. Further investigation of this locus is now warranted to uncover the mechanisms via which CACNA1A affects individual susceptibility to XFS.

Online Methods

Patient recruitment

Detailed information on all XFS sample collections can be found in Supplementary note. All patients and controls were enrolled into the study following informed consent and ethical approval from the relevant national and regional institutional review boards for each sample collection. DNA was extracted from patient blood samples using standard, well-described laboratory procedures for genetic analysis.

Genotyping

For the GWAS discovery stage, genome-wide genotyping was performed using the Illumina OmniExpress beadchips, following manufacturer's instructions (see URLs). For validation (Stage 1), genotyping was performed using the Sequenom MassArray platform (see URLs). For replication (Stage 2), genotyping was performed using Applied Biosystems Taqman probes (see URLs) for India, Germany, Italy, China, Iran, Poland, and Argentina. The Australian replication collection had GWAS genotyping on all cases and controls using Illumina genome-wide arrays, and *CACNA1A* rs4926244 was directly genotyped from the GWAS arrays. We perform cross-platform concordance checks and verify >99.9% concordance of genotypes for SNP markers of interest reported here (e.g. rs4926244).

Statistical analysis

Stringent quality control filters were used to remove poorly performing samples and SNP markers in both the GWAS discovery and validation phases. The SNPs with call rates of less than 95%, minor allele frequency of less than 1 percent, or showing significant deviation from Hardy-Weinberg Equilibrium (*P*-value for deviation $< 1 \times 10^{-6}$) were removed from further statistical analysis. Likewise, samples with an overall genotyping success rate of less than 95% were removed from further analysis. The remaining samples were then subjected to biological relationship verification by using the principle of variability in allele sharing. Identity-by-state information was derived using PLINK (see URLs). For those pairs of individuals who showed evidence of cryptic relatedness (possibly either due to duplicated or biologically related samples), we removed the sample with the lower call rate before performing principal component (PC) analysis. PC analysis was undertaken to account for spurious associations resulting from ancestral differences of individual SNPs and PC plots were performed using the R statistical program package (see URLs). For the GWAS discovery stage, all XFS cases had genetically matched controls as visualized spatially on PC analysis (Supplementary Figures 11a and 11b). A total of 581,023 autosomal SNPs passed quality filters for call rate and minor allele frequency (see **Methods**) and were included for further analysis. Genotypes were contrasted between XFS cases and controls using logistic regression, with adjustments for the top 6 principal components of genetic ancestry to further minimize confounding due to cryptic population stratification. We did not observe any evidence of genomic inflation ($\lambda gc = 1$; Supplementary Figure 12), suggesting that the association results were not confounded by external artefacts such as genetic mismatch between cases and controls. Crucially, we did not observe any deviation or dispersion of test statistics when patients with XFS without glaucoma were compared to patients with exfoliation glaucoma (Supplementary Figure 13). This suggests that our primary analysis approach in combining all XFS patients into an overall case group is valid.

For the GWAS discovery, validation, and replication stages, analysis of association with XFS disease status was carried out using allele-based score tests (1 degree of freedom), which models additive effects of the minor allele on disease risk. For the GWAS discovery stage, we incorporated the top six principal components of genetic stratification into the logistic regression model while performing the analysis for association to minimize the effect of residual population stratification. As the follow up validation (Stage 1) and replication (Stage 2) phases only tested a limited number of genetic markers, we were unable to adjust for population stratification in these follow up sample collections. However, association tests were performed by site to minimize population stratification and then subsequently combined in meta-analysis as described below. All *P*-values reported here are two-tailed.

Meta-analysis was conducted using inverse variance weights for each sample collection, which calculates an overall Z-statistic, its corresponding *P*-value, and accompanying odds ratios for each SNP analyzed. The meta-analysis is performed under the fixed effects model[30]. Analysis of linkage disequilibrium was performed using the R software package (version 2.9.0) and associated rmeta and RColorBrewer analytical packages.

Genotype Imputation

Fine-scale imputation at *CACNA1A* was performed using all 1,484 XFS cases and 1,188 controls passing the standard GWAS QC checks. The imputation and phasing of genotypes were carried out using IMPUTE2 (see URLs) with cosmopolitan population haplotypes based on data from 2535 individuals from 26 distinct populations around the world obtained from the 1000 Genomes project Phase 3 (Jun 2014) release for reference panel construction. Imputed genotypes were called with an impute probability threshold of 0.90 with all other genotypes classified as missing. Additional quality control filters were applied to remove SNPs with a call rate of < 99% should the SNP have a minor allele frequency (MAF) below 5% in either cases or controls. For common SNPS with MAF above 5%, the filtering criteria were set at less than 95% call rate.

Power calculations

All statistical power calculations were performed as previously described[31]. We present these power calculations for each of the following conditions; a) GWAS discovery stage only, b) GWAS discovery plus stage 1 validation, and c) GWAS discovery plus stage 1 validation plus stage 2 replication (Supplementary Table 9).

Expression analysis

RT-PCR in human ocular tissues: Multiple transcript variants encoding different isoforms have been found for *CACNA1A*. Here we assessed for the presence of either of the two major transcripts known for *CACNA1A*, which encode 2506 and 2261 amino acid isoforms, $Ca_V2.1$ variant-1 and 2 ($Ca_V2.1$_V2 and $Ca_V2.1$_V1, NCBI Reference Sequences: NM_001127222.1/NP_001120694.1 and NM_001127221.1/NP_001120693.1). All of the known critical regulatory elements of the $Ca_V2.1$ C-terminal tail are included in both variants, but the polyQ domain is excluded from the short-tail $Ca_V2.1$_V1 isoform[32]. We utilized 5 pairs of primers spread across and common to both transcripts to assess the presence of either transcript in eye tissues (Supplementary Table 10) *CACNA1A* transcript expression was assessed by semi quantitative reverse transcription PCR (RT-PCR) using the above mentioned *CACNA1A* specific primers on total RNA extracted from a variety of ocular tissues (anterior sclera, cornea, iris, trabecular meshwork, lens capsule, retina, choroid, optic nerve head and optic nerve) with TRIzol® Reagent (Invitrogen, Carlsbad, California) in accordance with the manufacturer's protocol. First-strand cDNA synthesis was performed with SuperScript First-Strand Synthesis System for RT-PCR (Invitrogen, Carlsbad, California). Semi quantitative RT-PCR was performed according to manufacturer's protocol, with the SYBR® Green Master Mix (Invitrogen, Carlsbad, California) using the above *CACNA1A* primers. RT-PCR products were separated on a 2% agarose gel and visualized by ethidium bromide staining. The ubiquitously expressed beta-actin *(ACTB)* gene was amplified using specific primers (Supplementary Table 10) and used as amplification and normalizing control.

Western Blotting

Cell lines obtained from American Type Culture Collection (Manassas, VA, USA) were the human retinal pigment epithelial cell line (APRE19), human cervical adenocarcinoma cell

line (Hela S), human breast adenocarcinoma cell line (MCF7), and human embryonic kidney epithelial cell line (HEK 293). Human nonpigmented ciliary epithelial cell line (NPCE) is a kind gift from Prof. Miguel Coca-Prados from Yale School of Medicine. Human Trabecular Meshwork cell line (HTM) was purchased from PromoCell GmbH (Heidelberg, Germany). Cell lysates were obtained by lysing individual cell lines with lysis buffer (50 mM Tris-HCl, pH 8, 150 mM NaCl, 1.0% Nonidet P-40, 0.5% deoxycholate, 0.1% SDS, 0.2 mM $NaVO_4$, 10 mM NaF, 0.4 mM EDTA, and 10% glycerol). SDS-PAGE resolved proteins were transferred to Hybond-C Extra nitrocellulose membranes (Amersham Life Science Inc., Arlington Heights, IL, USA). Membranes were blocked by 5% nonfat milk, 0.1% Tween 20 in Tris-buffered saline (20 mM Tris-HCl, pH 7.6, 150 mM NaCl) for 1 h before incubation with CACNA1A (1:1000) from Abcam Inc. (Cambridge, MA, USA), Actin-horseradish peroxidase (HRP) (1:50000) from Santa Cruz Biotechnology (Dallas, TX, USA). Blocking and blotting of antibodies were performed in 10% horse serum (Sigma-Aldrich Corp., St. Louis, MO, USA), 0.1% Tween 20 in phosphate-buffered saline for 1 h. The bound primary antibodies were detected by horseradish peroxidase-conjugated secondary antibodies (GE Healthcare Biosciences, Pittsburgh, PA, USA), and visualized by Luminata Forte Western HRP substrate (Millipore, Bedford, MA, USA).

Immunofluorescence Confocal Microscopy

Immunofluorescence confocal microscopy was performed on antigen retrieved 4μm paraffin sections. Blocking of tissue sections was performed with blocking buffer (10% FBS, 0.1% PBS-Tween; 1x pen/strep) for 1 hour at RT. CACNA1A (Abcam Inc., Catalog[#]: Ab81011 from Abcam) and LOXL1 (ABNOVA, Catalog [#] : H00004016-B01P from Abnova) antibodies were diluted at 1:300 ratio with blocking buffer and incubated overnight at 4°C. Secondary FITC (1:300) or Cy3 (1:300) labeled anti-mouse or anti-rabbit antibodies (Jackson Laboratories, Westgrove, PA, USA) were also diluted in blocking buffer and incubated at RT for 1 hour followed by application of Vectashield with 4′,6-diamidino-2-phenyl-indole (DAPI) (Vector Laboratories, Burlingame, CA, USA). Cover-slips were then used to overlay the sections and stored in the dark at 4°C until viewing with Olympus Fluoview 1000 confocal microscope (Olympus Optical Co. Ltd., Tokyo, Japan).

Immunohistochemistry

A total of 7 archival enucleated globes were retrieved for IHC analysis with CACNA1A (1:50) (Abcam Inc., Cambridge, MA, USA) and LOXL1 (1:50) (ABNOVA, Taipei, Taiwan) antibodies. Three human eye globes from Saudi Arabia and 1 from Denmark with a history of advanced XFS were obtained courtesy of Deepak Edward (KKESH, Riyadh Saudi Arabia) and Steffen Heegaard (University of Copenhagen, Denmark) respectively. Three additional eyes from Singapore (SGH-SNEC Ophthalmic pathology service, SGH Pathology) that were exenterated for other external pathological diagnoses that did not involve the globe were used as non-XFS controls. Immunohistochemistry (IHC) analysis was performed according to our previously published protocol[33]. In brief, paraffin sections were cut at 4μm and placed on coated slides. Immunohistochemistry was performed using the Leica Bond Polymer Refine detection kit DS9800 (Leica Microsystems GmbH, Wetzlar,

[#]Members of consortia and study groups are listed in the Supplementary Note.

Germany). Slides were heated for 20 minutes at 60°C and then loaded onto the Leica Bond III autostainer for immunohistochemical staining. Staining on the autostainer consisted of dewaxing, antigen retrieval using Leica Bond ER2 solution for 20mins at 100°C, antibody incubation for 20minutes at room temperature followed by staining using the Bond polymer refine kit. Polymeric alkaline phosphatase-AP linker antibody conjugate system (Vision Biosystems, Norwell, MA, USA) and counterstaining with haematoxylin were applied for visualization, after which the slides were dehydrated and cover-slipped.

Immunofluorescence confocal microscopy in mice

C57BL/6J and B6(Cg)-Tyrc-2J/J mice were obtained from The Jackson Laboratory production facility. Mice were housed with a 14-hour-light/10-hour-dark cycle, under the same conditions as previously described[34]. All experiments were performed in compliance with the ARVO statement for use of animals in ophthalmic and vision research and approved by The Jackson Laboratory Animal Care and Use Committee. Adult mice were deeply anesthetized and perfused with 1X phosphate buffered saline (PBS) and eyes were enucleated. Fresh tissue was frozen in optimal cutting temperature (OCT) compound frozen by liquid nitrogen cooled isopentane and stored at −80°C or eyes were fixed overnight in 4% paraformaldehyde. Fixed eyes were cyroprotected in 30% sucrose, rinsed in 1X PBS and frozen in OCT for sectioning. Eyes were cut into 12 μm sections. Primary antibodies used to stain sections included anti-CACNA1A (1:500, Millipore, Billerica, MA, USA), anti-Endomucin (EMCN; 1:500; eBioscience, San Diego, CA, USA), and anti-smooth muscle Actin (ACTA2; 1:500; Abcam, Cambridge, MA, USA). Alexafluor secondary antibodies from Invitrogen were used to label by immunofluorescence. Sections were desiccated, washed in 1X PBS with 0.5% Triton and incubated with primary antibodies overnight. Sections were subsequently washed in 1X PBS and incubated with secondary antibodies for 60 minutes. DAPI was used to stain nuclei. For each experiment, at least four sections from four eyes were assessed. Microscopy was performed on the Axio Imager (Zeiss).

Supplementary Material

Refer to Web version on PubMed Central for supplementary material.

Authors

Tin Aung[1,2,3,*], Mineo Ozaki[*,4,34], Takanori Mizoguchi[*,5], R Rand Allingham[6,*], Zheng Li[7], Aravind Haripriya[8], Satoko Nakano[9], Steffen Uebe[10], Jeffrey M. Harder[11], Anita S.Y. Chan[1,2], Mei Chin Lee[1], Kathryn P. Burdon[12,13], Yury S. Astakhov[14], Khaled K. Abu-Amero[15,16], Juan C. Zenteno[17,18], Yildirim Nilgün[19], Tomasz Zarnowski[20], Mohammad Pakravan[21], Leen Abu Safieh[22], Liyun Jia[23], Ya Xing Wang[24], Susan Williams[25], Daniela Paoli[26], Patricio G Schlottmann[27], Lulin Huang[28,29,30], Kar Seng Sim[7], Jia Nee Foo[7], Masakazu Nakano[31], Yoko Ikeda[32], Rajesh S Kumar[33], Morio Ueno[32], Shin-ichi Manabe[34], Ken Hayashi[34], Shigeyasu Kazama[35], Ryuichi Ideta[36], Yosai Mori[37], Kazunori Miyata[37,38], Kazuhisa Sugiyama[39], Tomomi Higashide[39], Etsuo Chihara[40], Kenji Inoue[41], Satoshi Ishiko[42], Akitoshi Yoshida[43], Masahide Yanagi[44], Yoshiaki Kiuchi[44], Makoto Aihara[45], Tsutomu Ohashi[46], Toshiya Sakurai[47], Takako Sugimoto[38], Hideki

Chuman[38], Fumihiko Matsuda[48], Kenji Yamashiro[49], Norimoto Gotoh[49], Masahiro Miyake[48,49], Sergei Y. Astakhov[14], Essam A. Osman[15], Saleh A. Al-Obeidan[15], Ohoud Owaidhah[21], Leyla Al-Jasim[21], Sami Al Shahwan[21], Rhys A. Fogarty[12], Paul Leo[50], Yaz Yetkin[19], Çilingir Oğuz[19], Mozhgan Rezaei Kanavi[21], Afsaneh Naderi Beni[21], Shahin Yazdani[21], Evgeny L. Akopov[14], Kai-Yee Toh[7], Gareth R Howell[11], Andrew C. Orr[51], Yufen Goh[7], Wee Yang Meah[7], Su Qin Peh[7], Ewa Kosior-Jarecka[20], Urszula Lukasik[20], Mandy Krumbiegel[10], Eranga N Vithana[1], Tien Yin Wong[1,2,3], Yutao Liu[52,53], Allison E. Ashley Koch[52], Pratap Challa[6], Robyn M Rautenbach[54], David A. Mackey[55], Alex W Hewitt[13,56], Paul Mitchell[57], Jie Jin Wang[57], Ari Ziskind[54], Trevor Carmichael[25], Rangappa Ramakrishnan[8], Kalpana Narendran[8], Rangaraj Venkatesh[8], Saravanan Vijayan[58], Peiquan Zhao[59], Xueyi Chen[60], Dalia Guadarrama-Vallejo[17,18], Ching Yu Cheng[1,3], Shamira A Perera[1,2], Rahat Husain[1,2], Su-Ling Ho[61], Ulrich-Christoph Welge-Luessen[62], Christian Mardin[62], Ursula Schloetzer-Schrehardt[62], Axel M. Hillmer[63], Stefan Herms[64,65,66,67], Susanne Moebus[68], Markus M. Nöthen[64,65], Nicole Weisschuh[69], Rohit Shetty[33], Arkasubhra Ghosh[1,70], Yik Ying Teo[7,71], Matthew A Brown[50], Ignacio Lischinsky[72], The Blue Mountains Eye Study GWAS team[73], Wellcome Trust Case Control Consortium[2,73], Jonathan G Crowston[56,74], Michael Coote[56,74], Bowen Zhao[22], Jinghong Sang[23], Nihong Zhang[23], Qisheng You[24], Vera Vysochinskaya[75], Panayiota Founti[76], Anthoula Chatzikyriakidou[77], Alexandros Lambropoulos[77], Eleftherios Anastasopoulos[76], Anne L Coleman[78], M Roy Wilson[79], Douglas J Rhee[80], Jae Hee Kang[81], Inna May-Bolchakova[82], Steffen Heegaard[83,84], Kazuhiko Mori[32], Wallace L.M. Alward[85,86], Jost B Jonas[87], Liang Xu[24], Jeffrey M Liebmann[88], Balram Chowbay[89], Elke Schaeffeler[90], Matthias Schwab[90,91,92], Fabian Lerner[93], Ningli Wang[23], Zhenglin Yang[28,29,30], Paolo Frezzotti[94], Shigeru Kinoshita[32], John H. Fingert[85,86], Masaru Inatani[95], Kei Tashiro[31], André Reis[10], Deepak P. Edward[22,96], Louis R. Pasquale[80,81], Toshiaki Kubota[9], Janey L. Wiggs[80,**], Francesca Pasutto[10,**], Fotis Topouzis[76,**], Michael Dubina[14,75,**], Jamie E. Craig[12,**], Nagahisa Yoshimura[49,**], Periasamy Sundaresan[58,**], Simon W.M. John[11,**], Robert Ritch[97,**], Michael A Hauser[6,52,**], and Chiea-Chuen Khor[3,7,**]

Affiliations

[1]Singapore Eye Research Institute, 11 Third Hospital Avenue, Singapore 168751 [2]Singapore National Eye Center, 11 Third Hospital Avenue, Singapore 168751 [3]Department of Ophthalmology, Yong Loo Lin School of Medicine, National University of Singapore [4]Ozaki Eye Hospital, 1-15, Kamezaki, Hyuga, Miyazaki 883-0066 Japan [5]Mizoguchi Eye Hospital, 6-13 Tawara-machi, Sasebo, Nagasaki, Japan 857-0016 [6]Department of Ophthalmology, Duke University Eye Center, Durham, NC [7]Division of Human Genetics, Genome Institute of Singapore [8]Intraocular Lens and Cataract Clinic, Aravind Eye Hospital, Madurai, India [9]Department of Ophthalmology, Oita University Faculty of Medicine [10]Institute of Human Genetics, Friedrich-Alexander-Universität Erlangen-Nürnberg, Germany [11]The Howard Hughes Medical Institute, the Jackson Laboratory 600 Main Street, Bar Harbor, ME 04609 [12]Department of Ophthalmology, Flinders University,

Adelaide, SA, Australia [13]Menzies Institute for Medical Research, University of Tasmania [14]Department of Ophthalmology, First Pavlov State Medical University of St. Petersburg, 6/8 L'va Tolstogo Street, 197022 St. Petersburg, Russia [15]Department of Ophthalmology, College of Medicine, King Saud University, Riyadh, Saudi Arabia [16]Department of Ophthalmology, College of Medicine, University of Florida, Jacksonville, FL, USA [17]Genetics Department, Institute of Ophthalmology "Conde de Valenciana", Mexico [18]Biochemistry Department, Faculty of Medicine, UNAM, Mexico City, Mexico [19]Department of Ophthalmology, Eskisehir Osmangazi University, Meselik, Eskisehir, Turkey [20]Department of Diagnostics and Microsurgery of Glaucoma, Medical University, Lublin, Poland, Chmielna 1, 20-079 Lublin, Poland [21]Ophthalmic Research Center, Ophthalmology department, Labbafinejad Medical Center, Shahid Beheshti University of Medical Sciences, Tehran, Iran [22]King Khaled Eye Specialist Hospital, Riyadh, Kingdom of Saudi Arabia [23]Beijing Ophthalmology & Visual Sciences Key Laboratory, Beijing Tongren Eye Centre, Beijing Tongren Hospital, Capital Medical University, Beijing, China [24]Beijing Institute of Ophthalmology, Beijing Tongren Hospital, Capital University of Medical Science, Beijing, China [25]Division of Ophthalmology, Department of Neurosciences, University of the Witwatersrand, Johannesburg, South Africa [26]Department of Ophthalmology, Monfalcone Hospital, Gorizia, Italy [27]Organización Médica de Investigación, Uruguay 725 – PB, Buenos Aires (C1015ABO) Argentina [28]Sichuan Provincial Key Laboratory for Human Disease Gene Study, Hospital of the University of Electronic Science and Technology of China and Sichuan Provincial People's Hospital, Chengdu, China [29]School of Medicine, University of Electronic Science and Technology of China, Chengdu, China [30]Sichuan Translational Medicine Hospital, Chinese Academy of Sciences, Chengdu, China [31]Department of Genomic Medical Sciences, Kyoto Prefectural University of Medicine, Kyoto, Japan [32]Department of Ophthalmology, Kyoto Prefectural University of Medicine, Kyoto, Japan [33]Glaucoma services, Narayana Nethralaya Eye Hospital, 121/C, Chord Road, Rajajinagar, 1st R Block, Bangalore 560 010, India [34]Hayashi Eye Hospital, 4-23-35, Hakataekimae, Hakata-ku, Fukuoka, Japan [35]Shinjo Eye Clinic, 889-1,Mego, Simokitakatamachi, Miyazaki-shi, Miyazaki 880-0035,Japan [36]Ideta Eye Hospital, Kumamoto, Japan [37]Miyata Eye Hospital, 6-3, Kurahara, Miyakonojo, Miyazaki 885-0051 Japan [38]Department of Ophthalmology, Faculty of Medicine, University of Miyazaki, Miyazaki, Japan [39]Department of Ophthalmology and Visual Science, Kanazawa University Graduate School of Medical Science, Kanazawa University, 13-1 Takara-machi, Kanazawa, 920-8641, Japan [40]Sensho-kai Eye Institute, Minamiyama 50-1, Iseda, Uji, Kyoto 611-0043, Japan [41]Inouye Eye Hospital, Tokyo, Japan [42]Department of Medicine and Engineering Combined Research Institute, Asahikawa Medical University, Asahikawa, Japan [43]Department of Ophthalmology, Asahikawa Medical University, Asahikawa, Japan [44]Department of Ophthalmology and Visual Science, Hiroshima University, Hiroshima, Japan [45]Yotsuya Shirato Eye Clinic, Tokyo, Japan [46]Ohashi eye center, Kita1-1 Hondori6 Shiroishi-ku Sapporo 003-0027 Japan [47]Tane Memorial Eye Hospital, Osaka [48]Center for Genomic Medicine/Inserm U.

852, Kyoto University Graduate School of Medicine, Kyoto, Japan [49]Department of Ophthalmology and Visual Sciences, Kyoto University Graduate School of Medicine, Kyoto, Japan [50]University of Queensland Diamantina Institute, Translational Research Institute, Princess Alexandra Hospital, Brisbane, Qld, Australia [51]Department of Ophthalmology and Visual Sciences, Dalhousie University, Halifax, Canada [52]Department of Medicine, Duke University Medical Center, Durham, North Carolina [53]Department of Cellular Biology and Anatomy, Georgia Regents University, Augusta, Georgia [54]Division of Ophthalmology, Faculty of Medicine and Health Sciences, University of Stellenbosch, Cape Town, South Africa [55]Centre for Ophthalmology and Visual Science, Lions Eye Institute, University of Western Australia, Perth, Australia [56]Centre for Eye Research Australia (CERA), University of Melbourne, Royal Victorian Eye and Ear Hospital, Melbourne, Victoria, Australia [57]Centre for Vision Research, Department of Ophthalmology and Westmead Millennium Institute, University of Sydney, NSW Australia [58]Department of Genetics, Aravind Medical Research Foundation, Madurai, India [59]Department of Ophthalmology, Xin Hua Hospital affiliated to Shanghai Jiao Tong University, School of Medicine, No. 1665, Kongjiang Road, Shanghai 200092, China [60]Department of Ophthalmology, the First Affiliated Hospital of Xinjiang Medical University, Urumchi 830054, Xinjiang Uygur Autonomous Region, China [61]National Healthcare Group Eye Institute, Tan Tock Seng Hospital, Singapore [62]Department of Ophthalmology, Friedrich-Alexander-Universität Erlangen-Nürnberg, Germany [63]Cancer Therapeutics and Stratified Oncology, Genome Institute of Singapore [64]Institute of Human Genetics, University of Bonn, Bonn, Germany [65]Department of Genomics, Life & Brain Center, University of Bonn, Bonn, Germany [66]Division of Medical Genetics, University Hospital, Basel, Switzerland [67]Human Genetics Research Group, Department of Biomedicine, University of Basel, Basel, Switzerland [68]Institute for Medical Informatics, Biometry and Epidemiology, University Hospital of Essen, University Duisburg-Essen, Essen, Germany [69]University Eye Hospital, Wuerzburg, Germany [70]Genes, Repair and Regeneration in Ophthalmic Workstation Research Lab, Narayana Nethralaya Foundation, Bangalore, India [71]Saw Swee Hock School of Public Health, National University of Singapore, Singapore [72]Centro Oftalmologico Lischinsky, Junin 692, Tucuman (4000) – Argentina [74]Department of Ophthalmology, University of Melbourne [75]St. Petersburg Academic University, 8/3 Klopina Street, 194021 St. Petersburg, Russia [76]Department of Ophthalmology, Faculty of Medicine, Aristotle University of Thessaloniki, AHEPA Hospital, Thessaloniki, Greece [77]Department of Biology and Genetics, Faculty of Medicine, Aristotle University of Thessaloniki, Greece [78]Center for Community Outreach and Policy, Stein Eye Institute, David Geffen School of Medicine at UCLA, Los Angeles, CA 90095 United States [79]Wayne State University, Detroit, 48202, United States [80]Department of Ophthalmology, Harvard Medical School, Massachusetts Eye and Ear Infirmary, Boston, Massachusetts, United States of America [81]Channing Division of Network Medicine, Brigham and Women's Hospital, Boston, Massachusetts, United States of America [82]Ophthalmology Department, Military Hospital Begin, Paris, France [83]Eye

Pathology Institute, Department of Neuroscience and Pharmacology, University of Copenhagen, Copenhagen, Denmark [84]Department of Ophthalmology, Glostrup University Hospital, Glostrup, Denmark [85]Stephen A. Wynn Institute for Vision Research, University of Iowa, USA [86]Department of Ophthalmology and Visual Sciences, Carver College of Medicine, University of Iowa, Iowa City [87]Department of Ophthalmology, Medical Faculty Mannheim of the Ruprecht-Karls-University Heidelberg, Germany [88]New York University School of Medicine; Manhattan Eye, Ear and Throat Hospital, New York [89]Division of Medical Sciences, Humphrey Oei Institute of Cancer Research, National Cancer Centre of Singapore [90]Dr. Margarete Fischer-Bosch-Institute of Clinical Pharmacology, Stuttgart, and University Tuebingen, Germany [91]Department of Clinical Pharmacology, University Hospital, Tuebingen, Germany [92]German Cancer Consortium (DKTK), German Cancer Research Center, Heidelberg, Germany [93]Fundacion para el Estudio del Glaucoma, Marcelo T de Alvear 2010 - 2A Buenos Aires (C1122AAF) Argentina [94]Department of Surgery, Section of Ophthalmology, University of Siena, Siena, Italy [95]Department of Ophthalmology, Faculty of Medical Science, University of Fukui, 23-3 Shimoaizuki, Matsuoka, Eiheiji, Yoshida, Fukui, 910-1193, Japan [96]Wilmer Eye Institute, Johns Hopkins University School of Medicine, Baltimore, Maryland, United States of America [97]Einhorn Clinical Research Center, New York Eye and Ear Infirmary of Mount Sinai, New York, NY, United States of America

Acknowledgments

The authors thank the staff and participants of all studies for their important contributions. We thank Khai-Koon Heng, Xiao-Yin Chen, Hui-Meng Soo, Shi-Qi Mok, Andrea Jamuth, Nicole Foxworth and Monika Elbl for technical assistance. This research was funded by the Biomedical Research Council, Agency for Science, Technology and Research, Singapore. J.L.W. acknowledges support from the National Institutes of Health/National Eye Institute grants (NIH/NEI R01 EY020928 and NIH/NEI P30 EY014104). SWMJ acknowledges support from EY11721 and is an Investigator of the Howard Hughes Medical Institute. L.R.P. acknowledges support from a Harvard Medical School Distinguished Ophthalmology Scholar Award and the Harvard Glaucoma Center of Excellence. J.H.F. acknowledges support from the National Institutes of Health/National Eye Institute grants (EY023512 and EY018825). Zhenglin Yang acknowledges support from the National Natural Science Foundation of China (81025006, and 81170883), as well as from the Department of Science and Technology of Sichuan Province, China (2012SZ0219 (Z.Y.) and 2011jtd0020 (Z.Y.). M. Schwab acknowledges support from the Robert Bosch Stiftung, Stuttgart, Germany and The German Cancer Consortium (DKTK), Germany. The Australian case cohort was funded by grants from the Ophthalmic Research Institute of Australia and the National Health and Medical Research Council (NHMRC) project #535044. The Thessaloniki Eye Study was co-funded by the European Union (European Social Fund) and Greek national funds under the Act “Aristia” of the Operational Program “Education and Lifelong Learning” (see Supplementary Note). The Blue Mountains Eye Study (BMES) GWAS and genotyping costs was supported by Australian NHMRC, Canberra Australia (NHMRC project grant IDs 512423, 475604 and 529912), and the Wellcome Trust, UK as part of Wellcome Trust Case Control Consortium 2 (A Viswanathan, P McGuffin, P Mitchell, F Topouzis, P Foster, grant IDs 085475/B/08/Z and 085475/08/Z). K.P.B. is an NHMRC Senior Research Fellow and J.E.C. is an NHMRC Practitioner Fellow. M.A.B. is a NHMRC Principal Research Fellow. A.W.H. is a NHMRC Peter Doherty Fellow.

References for main text

1. Schlotzer-Schrehardt U, Naumann GO. Ocular and systemic pseudoexfoliation syndrome. Am J Ophthalmol. 2006; 141:921–937. [PubMed: 16678509]
2. Ritch R, Schlotzer-Schrehardt U. Exfoliation syndrome. Surv Ophthalmol. 2001; 45:265–315. [PubMed: 11166342]

3. Thorleifsson G, et al. Common sequence variants in the LOXL1 gene confer susceptibility to exfoliation glaucoma. Science. 2007; 317:1397–400. [PubMed: 17690259]
4. Chen H, et al. Ethnicity-based subgroup meta-analysis of the association of LOXL1 polymorphisms with glaucoma. Mol Vis. 2010; 16:167–77. [PubMed: 20142848]
5. Fingert JH, et al. LOXL1 mutations are associated with exfoliation syndrome in patients from the midwestern United States. Am J Ophthalmol. 2007; 144:974–975. [PubMed: 18036875]
6. Hayashi H, Gotoh N, Ueda Y, Nakanishi H, Yoshimura N. Lysyl oxidase-like 1 polymorphisms and exfoliation syndrome in the Japanese population. Am J Ophthalmol. 2008; 145:582–585. [PubMed: 18201684]
7. Fan BJ, et al. DNA sequence variants in the LOXL1 gene are associated with pseudoexfoliation glaucoma in a U.S. clinic-based population with broad ethnic diversity. BMC Med Genet. 2008; 9:5. [PubMed: 18254956]
8. Yang X, et al. Genetic association of LOXL1 gene variants and exfoliation glaucoma in a Utah cohort. Cell Cycle. 2008; 7:521–4. [PubMed: 18287813]
9. Hewitt AW, et al. Ancestral LOXL1 variants are associated with pseudoexfoliation in Caucasian Australians but with markedly lower penetrance than in Nordic people. Hum Mol Genet. 2008; 17:710–6. [PubMed: 18037624]
10. Pasutto F, et al. Association of LOXL1 common sequence variants in German and Italian patients with pseudoexfoliation syndrome and pseudoexfoliation glaucoma. Invest Ophthalmol Vis Sci. 2008; 49:1459–63. [PubMed: 18385063]
11. Ozaki M, et al. Association of LOXL1 gene polymorphisms with pseudoexfoliation in the Japanese. Invest Ophthalmol Vis Sci. 2008; 49:3976–80. [PubMed: 18450598]
12. Fan BJ, et al. LOXL1 promoter haplotypes are associated with exfoliation syndrome in a U.S. Caucasian population. Invest Ophthalmol Vis Sci. 2011; 52:2372–8. [PubMed: 21212179]
13. Wolf C, et al. Lysyl oxidase-like 1 gene polymorphisms in German patients with normal tension glaucoma, pigmentary glaucoma and exfoliation glaucoma. J Glaucoma. 2010; 19:136–41. [PubMed: 19373106]
14. Lemmela S, et al. Association of LOXL1 gene with Finnish exfoliation syndrome patients. J Hum Genet. 2009; 54:289–97. [PubMed: 19343041]
15. Aragon-Martin JA, et al. Evaluation of LOXL1 gene polymorphisms in exfoliation syndrome and exfoliation glaucoma. Mol Vis. 2008; 14:533–41. [PubMed: 18385788]
16. Chen L, et al. Evaluation of LOXL1 polymorphisms in exfoliation syndrome in a Chinese population. Mol Vis. 2009; 15:2349–57. [PubMed: 19936304]
17. Mossbock G, et al. Lysyl oxidase-like protein 1 (LOXL1) gene polymorphisms and exfoliation glaucoma in a Central European population. Mol Vis. 2008; 14:857–61. [PubMed: 18483563]
18. Challa P, et al. Analysis of LOXL1 polymorphisms in a United States population with pseudoexfoliation glaucoma. Mol Vis. 2008; 14:146–9. [PubMed: 18334928]
19. Ramprasad VL, et al. Association of non-synonymous single nucleotide polymorphisms in the LOXL1 gene with pseudoexfoliation syndrome in India. Mol Vis. 2008; 14:318–22. [PubMed: 18334947]
20. Nakano M, et al. Novel common variants and susceptible haplotype for exfoliation glaucoma specific to Asian population. Sci Rep. 2014; 4:5340. [PubMed: 24938310]
21. Mori K, et al. LOXL1 genetic polymorphisms are associated with exfoliation glaucoma in the Japanese population. Mol Vis. 2008; 14:1037–40. [PubMed: 18552979]
22. Williams SE, et al. Major LOXL1 risk allele is reversed in exfoliation glaucoma in a black South African population. Mol Vis. 2010; 16:705–12. [PubMed: 20431720]
23. Krumbiegel M, et al. Genome-wide association study with DNA pooling identifies variants at CNTNAP2 associated with pseudoexfoliation syndrome. Eur J Hum Genet. 2011; 19:186–93. [PubMed: 20808326]
24. Rioux JD, et al. Genetic variation in the 5q31 cytokine gene cluster confers susceptibility to Crohn disease. Nat Genet. 2001; 29:223–8. [PubMed: 11586304]
25. Westra HJ, et al. Systematic identification of trans eQTLs as putative drivers of known disease associations. Nat Genet. 2013; 45:1238–43. [PubMed: 24013639]

26. Boyle AP, et al. Annotation of functional variation in personal genomes using RegulomeDB. Genome Res. 2012; 22:1790–7. [PubMed: 22955989]
27. Ward LD, Kellis M. HaploReg: a resource for exploring chromatin states, conservation, and regulatory motif alterations within sets of genetically linked variants. Nucleic Acids Res. 2012; 40:D930–4. [PubMed: 22064851]
28. Schlotzer-Schrehardt U, Kortje KH, Erb C. Energy-filtering transmission electron microscopy (EFTEM) in the elemental analysis of pseudoexfoliative material. Curr Eye Res. 2001; 22:154–62. [PubMed: 11402393]
29. Reinhardt DP, Ono RN, Sakai LY. Calcium stabilizes fibrillin-1 against proteolytic degradation. J Biol Chem. 1997; 272:1231–6. [PubMed: 8995426]
30. Willer CJ, Li Y, Abecasis GR. METAL: fast and efficient meta-analysis of genomewide association scans. Bioinformatics. 2010; 26:2190–1. [PubMed: 20616382]
31. Purcell S, Cherny SS, Sham PC. Genetic Power Calculator: design of linkage and association genetic mapping studies of complex traits. Bioinformatics. 2003; 19:149–50. [PubMed: 12499305]
32. Tsou WL, Soong BW, Paulson HL, Rodriguez-Lebron E. Splice isoform-specific suppression of the Cav2.1 variant underlying spinocerebellar ataxia type 6. Neurobiol Dis. 2011; 43:533–42. [PubMed: 21550405]
33. Lee MC, et al. Expression of the Primary Angle Closure Glaucoma (PACG) Susceptibility Gene PLEKHA7 in Endothelial and Epithelial Cell Junctions in the Eye. Invest Ophthalmol Vis Sci. 2014; 55:3833–41. [PubMed: 24801512]
34. Smith RS, et al. Haploinsufficiency of the transcription factors FOXC1 and FOXC2 results in aberrant ocular development. Hum Mol Genet. 2000; 9:1021–32. [PubMed: 10767326]

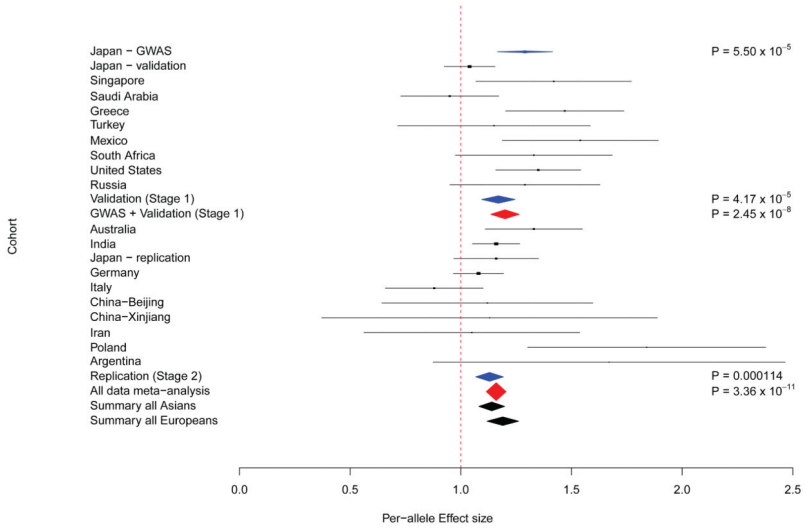

Figure 1.

Forest plot for the associations between *CACNA1A* rs4926244 and Exfoliation syndrome in discovery and follow up case-control collections. The black lines denote the 95% confidence intervals of the odds ratio for each collection. The diamonds denote summary results for the GWAS, Validation and Replication stages (blue), as well as the GWAS and Validation meta-analysis, and meta-analysis of data from all collections (red). Asian and European ethnic summaries are in black diamonds.

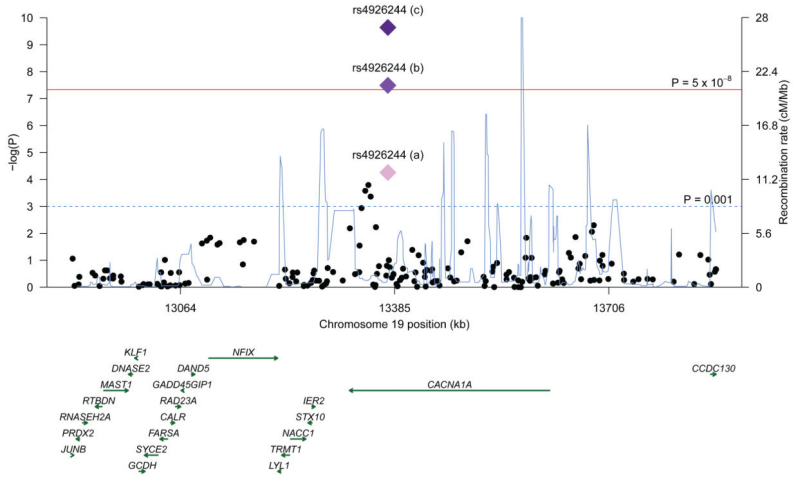

Figure 2.

Regional association and recombination rate plot for the *CACNA1A* rs4926244 locus. The left *y* axis represents –log10 *P* values for association with exfoliation syndrome and the right *y* axis represents the recombination rate. The *x* axis represents base-pair positions along the chromosome (human genome Build 37). The diamonds denote the summary of each experimental stage, a) for the GWAS discovery, b) for the meta-analysis between GWAS discovery and validation stages, and c) for the meta-analysis between GWAS discovery, validation, and replication stages.

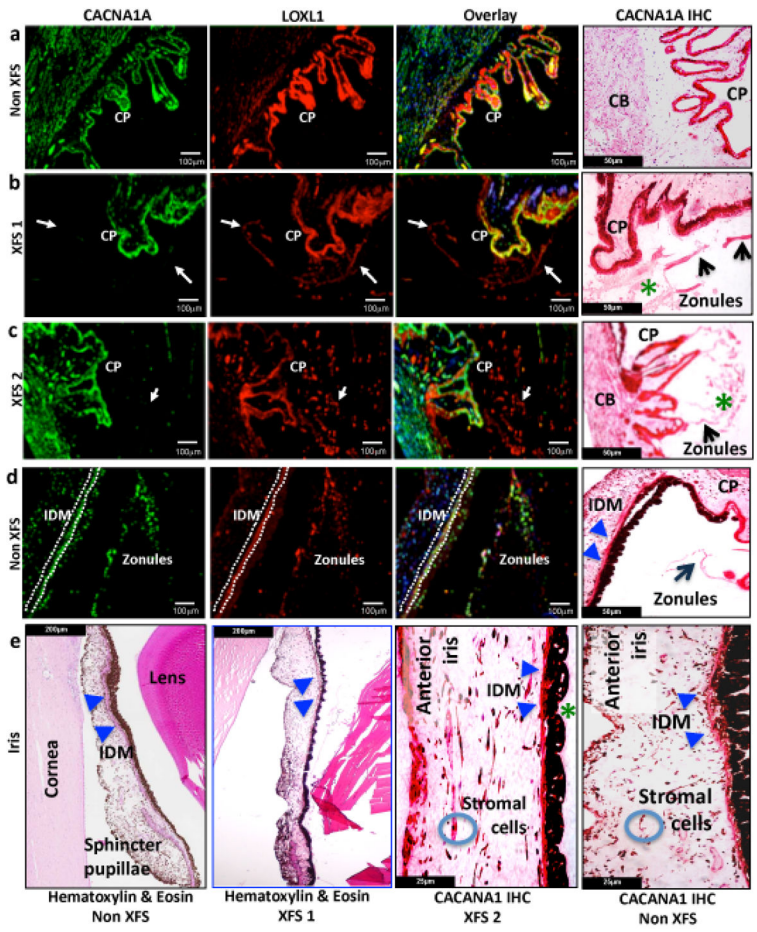

Figure 3.

CACNA1A and LOXL1 protein expression and light microscopic analysis in XFS and non-XFS control eyes. Immunolocalisation of CACNA1A in human non-XFS and XFS globes show CACNA1A positive immunoreactivity in the smooth musculature of the ciliary body (CB) and pigmented and non-pigmented ciliary process (CP) epithelium with variable staining in the zonules (Panels a to c: CACNA1A immunofluorescence (IF) panel; CACNA1A immunohistochemical (IHC) panel, 40x; zonules, white and black arrows; exfoliated material, green asterix). In contrast, LOXL1 immunoreactivity is present only in the exfoliated material and the CP epithelium, (LOXL1 IF panel; zonules, white arrows). Double immunofluorecence analysis shows colocalisation of CACNA1A and LOXL1 within the non-pigmented and pigmented epithelium of the CP but not in the CB smooth muscles or the zonules (IF overlay panel; zonules, white arrows). Light microscopy comparison of non-XFS and XFS irides show the typical XFS findings of exfoliated material (green asterix) on the posterior iris and atrophic iris pigment epithelium with possible atrophy of the iris dilator muscle (blue arrowheads) in XFS irides. The sphincter pupillae in both non-XFS and XFS shows negligible differences (H&E panels). CACNA1A positive immunoreactivity is also seen in the anterior iris border, iris stromal cells, the iris dilator (blue arrowheads, H&E and IHC panels) and sphincter muscles as well as the iris pigmented epithelium in both XFS and Non-XFS irides (Panel d & e: CACNA1A IF and CACNA1A IHC panels). Stromal cells are

highlighted by the blue circles. For CACNA1A, LOXL1, and overlay panels a) through to d), each unit on the scale bar represents 100 μm. For CACNA1A IHC panels a) to d), each unit on the scale bar represents 50 μm. For panel e) hematoxylin & eosin non-XFS as well as hematoxylin & eosin XFS1, each unit on the scale bar represents 200 μm. For panel e) CACNA1A IHC XFS2 as well as CACNA1A IHC non-XFS, each unit on the scale bar represents 25 μm.